



STRUT-AND-TIE MODELS FOR DEFORMATION OF REINFORCED CONCRETE BEAM-COLUMN JOINTS DEPENDENT ON PLASTIC HINGE BEHAVIOR OF BEAMS

Sung-gul HONG¹ and Soo-gon LEE²

SUMMARY

This paper presents a strut-and-tie model for evaluating deformation of reinforced concrete interior beam-column assemblages limited by shear failure of joint region. The effect of plastic hinge deformation of beams on shear strength of joint region is defined in terms of bond deterioration and softening of concrete compression. The strength and the limited deformation calculated by the proposed model are compared with available test results, showing good agreement. Since this proposed model depicts the stress flow not at ultimate, but at a required deformation level selected by practitioner, it can provide a clearer understanding of the relationship between the response of beam-column assemblages and the strength of the joint regions.

INTRODUCTION

Under lateral loading like seismic attack, beam-column joint is generally subject to many times higher shear forces than those of beams or columns adjacent to the joint. To insure the ductile response of beam-column assemblage, the shear strength of the joint should be guaranteed till the plastic hinges form at the beams and deform to the required level. Traditional design objective for reinforced concrete beam-column joint has been to treat it as though it were brittle. And the objective of capacity design philosophy is to design a beam-column joint that is stronger than the frame beams. An overstrength factor is used to create the probable demand and thereby attain a conservative design criterion for the beam-column joint. Current ACI code provisions [1] for beam-column joint provide the limitations for shear force and impractical details of reinforcement so that the joint shear failure may not curtail ductile response of structural frame. These limits of shear stress are also conservatively approximated values. Much of this apparent conservatism is caused by the uncertainty and complexity of load transfer mechanism within the joint.

It is generally admitted that the joint shear force is transferred by diagonal strut mechanism (Fig. 1(a)) and truss mechanism (Fig. 1(b)) [2]. However, there is some confusion with the determination of the contributions between two mechanisms. To validate the truss mechanism, bond resistance of the reinforcing bars of beam passing through the joint should be secured. Bond resistance, however, is likely

¹ Associate Professor, Seoul National University, Seoul, Korea. E-mail: sglhong@snu.ac.kr

² PhD. Student, Seoul National University, Seoul, Korea. E-mail: gon4ever@passmail.to

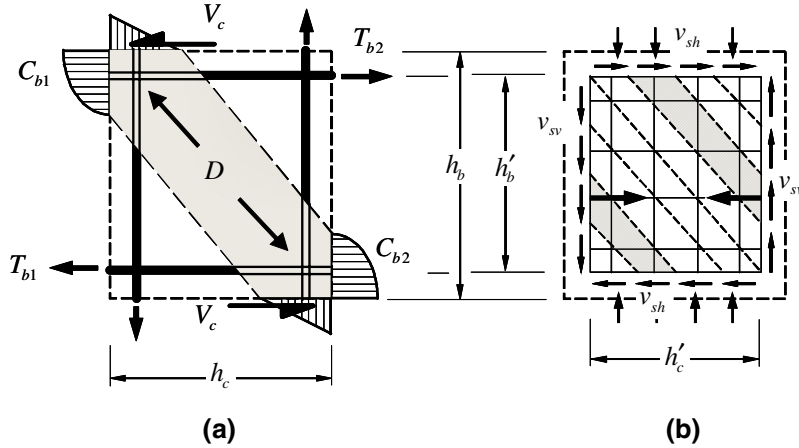


Fig. 1 Shear transfer mechanisms of internal beam-column joint (a) Diagonal strut mechanism (b) Truss mechanism

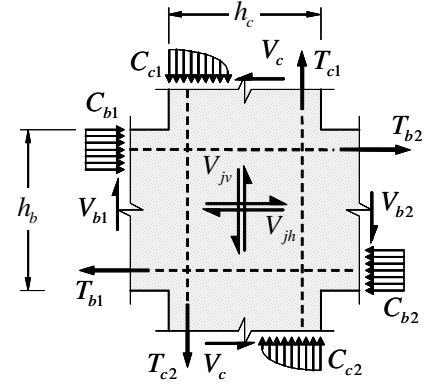


Fig. 2 Forces acting on interior beam-column joint

to decrease with plastic deformation of the bars. Modeling with only the diagonal strut mechanism induces a conservative solution for the shear carrying capacity of beam-column joint.

Hwang and Lee [3][4] proposed softened strut-and-tie models for exterior and interior beam-column joint, which determined the fractions of diagonal strut mechanism and truss mechanism according to the geometries of the joint, and considered the softening of diagonal strut. But, these models where truss mechanism depends on the joint geometries, could not explain the reduction of truss mechanism by the bond deterioration.

Shear strength of the joint region decreases as the deformation at the adjacent beams increases. The increase of plastic deformation of beam bars causes bond deterioration at the joint region and increases shear deformation of the joint resulting in the softening of concrete compression in the joint core. In this paper, the effects of plastic hinge deformation on the shear strength are considered for strut-and-tie models of interior beam-column joints. These proposed models provide a rational tool to determine the shear strength of interior beam-column joint related to the deformation of plastic hinges at the adjacent beams, and to estimate the system ductility limited by shear failure of the joint with that model vice versa.

CONSTRUCTION OF STRUT-AND-TIE MODEL

Shear force acting on interior beam-column joint

Forces acting on the interior beam-column joint under lateral loading are shown in Fig. 2 and the horizontal joint shear force acting on the joint core can be postulated as:

$$V_{jh} = T_{bl} + C_{b2} - V_c \quad (1)$$

where V_{jh} is the horizontal shear force on joint; T_{bl} is the tensile force of beam reinforcement at the right face of column; C_{b2} is the compressive force of beam flexural compression block at the left face of column; and V_c is shear force of column above the joint.

For the interior beam-column assemblage, plastic hinges are desired to form at beams near the column faces. Thereby, the yielding of reinforcing bars in the beams is assumed. Then, equilibrium conditions of the left-side beam at the column face allow compressive force C_{b2} to be substituted by tensile force T_{b2} .

$$V_{jh} = A_{s1}f_y + A_{s2}f_y - \frac{M_{u1} + M_{u2}}{h} \quad (2)$$

where A_{s1} and A_{s2} are the areas of tension reinforcement of right-side and left-side beams, respectively; f_y is the strength of reinforcing bars; M_{u1} and M_{u2} are the moment capacities of the beams; and h is inter-story height, that is the distance between the contraflexural points of upper and lower columns.

Definitions of deformation in joint

As a factor representing the plastic hinge deformation of beam, a required strain (ϵ_{req}) of main bars of beam at the column face is taken. The required strain is supposed to be a value postulated from the demand of plastic hinge deformation at design of beam ($\epsilon_{req} \geq \epsilon_y$).

Under the different state of the required strain of bars, distributions of strain along the horizontal chord within the joint region are proposed as shown in Fig. 3. Linear strain distributions of bars at tensile region are assumed and the ratio of strain change along the bar direction is calculated from the bond strength. Correlated distributions of bar stress and bond forces are demonstrated. In addition, expected stress fields of concrete compression are also depicted in accordance with the bond stress distributions. These are divided into three states that are before bond stress reaching the strength (State I, see Fig. 3(a)), after bond

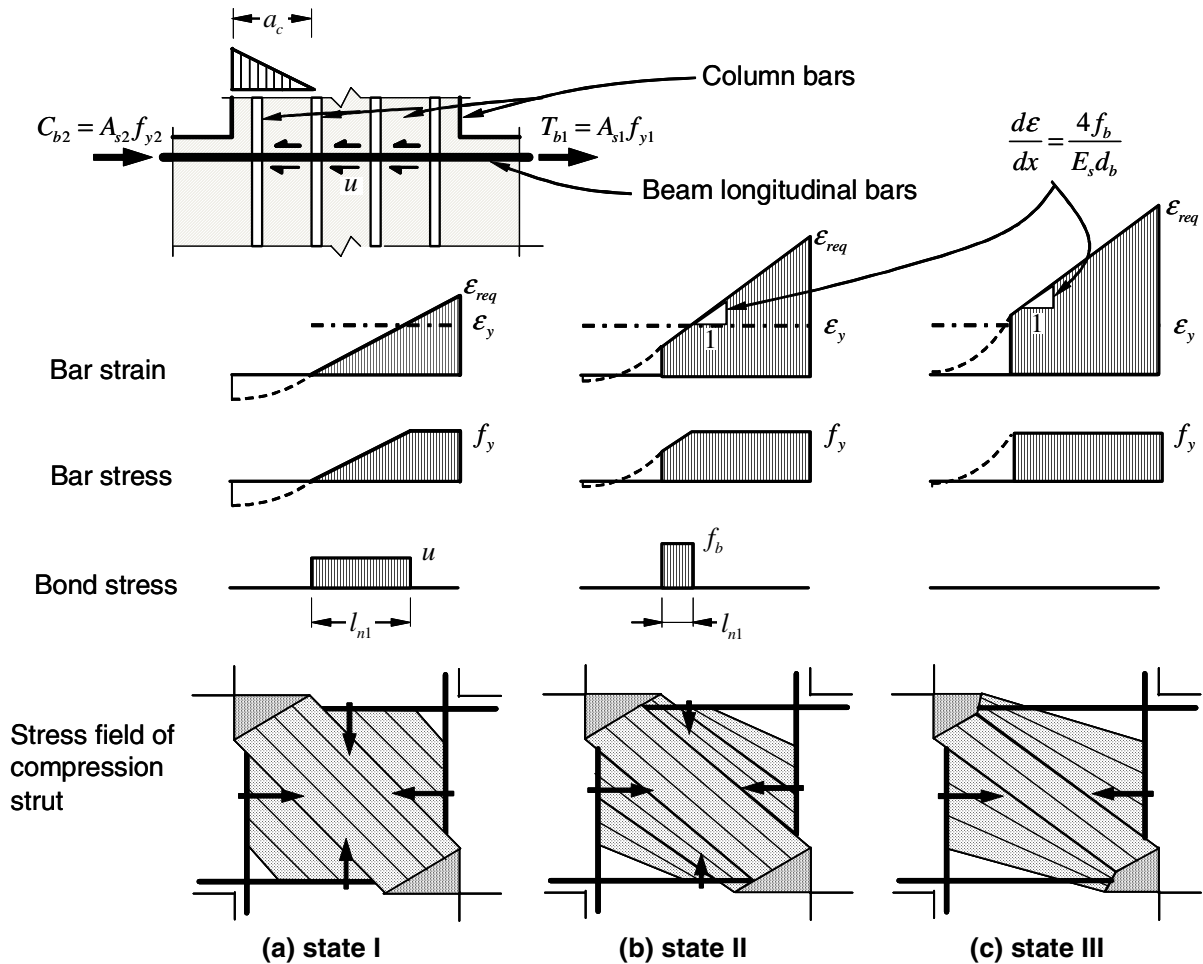


Fig. 3 Distributions of strain along the horizontal chord within the joint I

stress reaching the strength (State II, see Fig. 3(b)), and after bond force being lost (State III, see Fig. 3(c)). The slope of strain distribution along the horizontal chord (regard x -axis) is

$$\frac{d\varepsilon}{dx} \leq \frac{4f_b}{E_s d_b} \quad (3)$$

where the sign of equality is given at state II and state III (bond stress reaching the strength); f_b is bond strength; E_s is Elastic modulus of the reinforcing bars; and d_b is bar diameter.

From the horizontal strain distributions illustrated in Fig. 3, horizontal deformation of the joint can be calculated, and the average strain of joint core is determined. Fig. 4 shows the horizontal strain distribution of (a) top chord, (b) joint core, and (c) bottom chord. The average strain of top chord is

$$\varepsilon_h = \begin{cases} \frac{1}{2} \varepsilon_{req} \left(1 - \frac{a_c}{h_c} \right) - \frac{1}{2} \cdot \varepsilon_c \cdot \frac{a_c}{h_c} & \text{(state I)} \\ \left(\varepsilon_{req} - (h_c - a_c) \frac{2f_b}{E_s d_b} \right) \left(1 - \frac{a_c}{h_c} \right) - \frac{1}{2} \cdot \varepsilon_c \cdot \frac{a_c}{h_c} & \text{(state II or III)} \end{cases} \quad (4)$$

where, a_c is the depth of the compression zone in the column; and ε_c is the strain of beam compression block, which can be calculated from the tensile strain ε_{req} and neutral axis of the beam as follows:

$$\varepsilon_c = \varepsilon_{req} \frac{a_b}{(d - a_b)} \quad (5)$$

where, a_b is the depth of the compression zone in the beam; d is the distance from the top of compression zone to the centroid of tensile reinforcement at the beam. The average strain of bottom chord is calculated in the same manner, the average strain of the joint core is determined as the mean of the average strains of the top and the bottom chord.

Geometries of strut-and-tie model

A stress field for an interior beam-column joint is proposed as shown in Fig. 5(a) representing all the states of the required strain level, the strut-and-tie model is developed based on this stress field (See Fig. 5(b)). Though the compression force C_{b2} is not actually coincided with tensile force T_{b1} , the location of compression force is assumed at the location of main bars for simplicity. Strut angles of inclination α_1 and α_2 are defined as:

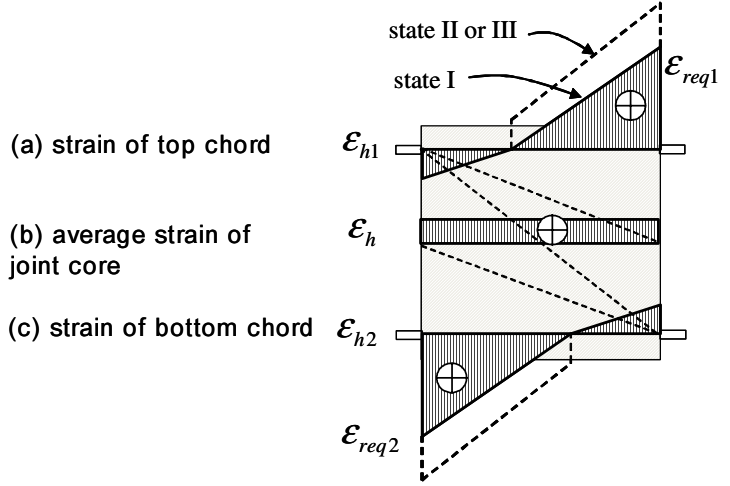


Fig. 4 Strain of horizontal chord

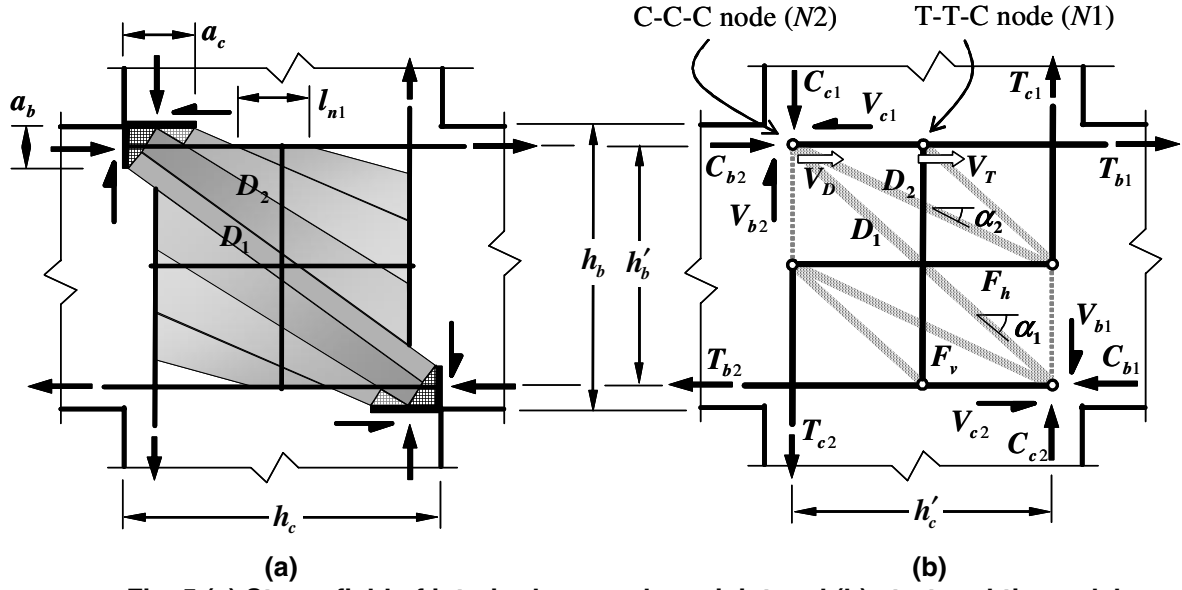


Fig. 5 (a) Stress field of interior beam-column joint and (b) strut-and-tie model

$$\tan \alpha_1 = \frac{h'_c}{h'_b} \quad (6)$$

$$\tan \alpha_2 = \frac{h'_c}{2h'_b} \quad (7)$$

where h'_c and h'_b are the distance between the longitudinal reinforcement in the column and beam, respectively. Regarding that beam near the column face reaches the flexural capacity (M_u), the depth of beam compression zone (a_b) is calculated as follows:

$$a_b = \frac{A_s f_y}{0.85 b_b f'_c} \quad (8)$$

where A_s is the area of tensile reinforcement of the beam; and b_b is the beam width. For the depth of compression zone of column (a_c), the equation approximated by Pauley and Priestley [5] is used as follows:

$$a_c = \left(0.25 + \frac{N}{h_c b_c f'_c} \right) h_c \quad (9)$$

where N is the axial force acting on the column; h_c and b_c are the thickness and width of column, respectively.

Effective strength of components

For determining the strength of the strut-and-tie model, the effective strength of components, involving struts, ties, and nodes should be defined based on the required strain level.

Struts and ties

Transversely cracked concrete in compression has been observed to have lower strength and stiffness than uniaxially compressed concrete. Constitutive equations of uniaxially compressive concrete have been derived considering the softening [6][7], and those have applied to the shear problems in reinforced concrete. The shear strength of joint is certainly governed by such softening of concrete in compression. For the strength of diagonal struts within the joint, the strength of compressed concrete with tensile strain in transversely direction, which is proposed in Modified Compression Field Theory, [6] is used. For simplicity, the direction of diagonal strut is assumed as the principal direction of compression.

$$f_{cd} = \frac{f'_c}{0.8 + 170\varepsilon_1} \leq f'_c \quad (10)$$

where ε_1 is an average principal tensile strain of cracked concrete. The principal tensile strain ε_1 can be obtained considering the horizontal strain ε_h , the vertical strain ε_v , and the principal compressive strain ε_2 based on the two-dimensional compatibility condition.

$$\varepsilon_1 + \varepsilon_2 = \varepsilon_h + \varepsilon_v \quad (11)$$

The principal compressive strain ε_2 reaches 0.002 from the assumption that the diagonal strut reaches the strength. The horizontal strain ε_h is in Eq. (4) and the vertical strain ε_v is

$$\varepsilon_v = V_t \tan \alpha_2 / h'_c \quad (12)$$

The strengths of horizontal tie (F_h) and vertical tie (F_v) are taken as the strength of the joint hoop bars, and column bars in joint core, respectively.

$$F_{yh} = A_{sh} f_y \quad (13)$$

$$F_{yv} = A_{sv} f_y \quad (14)$$

T-T-C nodal zone

Considering the bond deterioration within the joint, the effective strength of the T-T-C node (N1) is determined in accordance with the deformation states in Fig. 3. The bond stress (u) and the length of nodal zone (l_{n1}) resisting the shear can be determined. At each state, the bond stress and nodal zone length are

$$u = \begin{cases} \frac{d_b f_y}{4 l_{n1}} \left(\text{state I: } \varepsilon_{req} \leq \frac{4 f_b}{E_s d_b} (h_c - a_c) \right) \\ f_b \left(\text{state II: } \frac{4 f_b}{E_s d_b} (h_c - a_c) \leq \varepsilon_{req} \leq \varepsilon_y + \frac{4 f_b}{E_s d_b} (h_c - a_c) \right) \\ 0 \left(\text{state III: } \varepsilon_{req} \geq \varepsilon_y + \frac{4 f_b}{E_s d_b} (h_c - a_c) \right) \end{cases} \quad (15)$$

$$l_{n1} = \begin{cases} (h_c - a_c) \frac{\varepsilon_y}{\varepsilon_{req}} & \left(\text{state I: } \varepsilon_{req} \leq \frac{4f_b}{E_s d_b} (h_c - a_c) \right) \\ h_c - a_c - \frac{E_s d_b}{4 f_b} \varepsilon_{req} & \left(\text{state II: } \frac{4f_b}{E_s d_b} (h_c - a_c) \leq \varepsilon_{req} \leq \varepsilon_y + \frac{4f_b}{E_s d_b} (h_c - a_c) \right) \\ 0 & \left(\text{state III: } \varepsilon_{req} \geq \varepsilon_y + \frac{4f_b}{E_s d_b} (h_c - a_c) \right) \end{cases} \quad (16)$$

Accordingly, the shear transferring capacity of the T-T-C node (N1) is

$$V_{N1} = n\pi d_b l_{n1} f_b \quad (17)$$

where n is the number of tension reinforcing bars of beam passing through the joint; d_b is bar diameter.

C-C-C nodal zone

Basically nodal zone of C-C-C node (N2) is taken as triangular region surrounded by the compression zone of beam, column (a_b and a_c) and diagonal strut of the joint. For estimating the strength of C-C-C node (N2), it is considered that load path in the joint is divided into direct diagonal strut (D_1) and horizontal tie aided diagonal strut (D_2). Note that the indirect mechanism by strut (D_2) can be regarded as the confining effect of diagonal strut (D_1) by joint core reinforcement. Fig. 6 shows the C-C-C nodal zone to be composed of the end of strut D_1 and the end of D_2 . The compression force caused by bond force along the beam bars within the C-C-C nodal zone is also included in the strut D_2 . The bond strength (f_{bc}) in C-C-C node is assumed to be twice of the bond strength in T-T-C node (f_b).

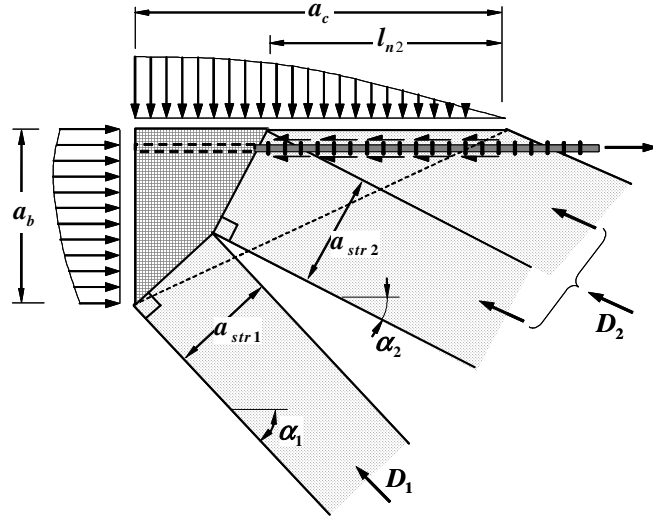


Fig. 6 Geometries within the C-C-C nodal zone (N2)

Regarding the stress of the strut D_2 as the capacity that is $a_{str2} b (0.85 f'_c)$ at the border of C-C-C node and strut D_2 , simultaneous equations with diagonal strut depths and the length carrying the bond stress within the C-C-C node are derived as:

$$n(\pi d_b) l_{n2} f_{bc} + a_{str2} b (0.85 f'_c) \cos \alpha_2 = D_2 \cos \alpha_2 \quad (18)$$

$$a_{str1} \sin \alpha_1 + a_{str2} \sin \alpha_2 = a_c - l_{t2} \quad (19)$$

$$a_{str1} \cos \alpha_1 + a_{str2} \cos \alpha_2 = a_b \quad (20)$$

From the simultaneous equations above, the depths of diagonal struts and bond length within the C-C-C node can be calculated as:

$$l_{n2} = \left\{ D_2 \cos \alpha_2 + \frac{b(0.85 f'_c)(a_c - a_b \tan \alpha_1)}{\tan \alpha_1 - \tan \alpha_2} \right\} / \left\{ n\pi d_b f_{bc} + \frac{b(0.85 f'_c)}{\tan \alpha_1 - \tan \alpha_2} \right\} \quad (21)$$

$$a_{str2} = (l_{n2} - a_c + a_b \tan \alpha_1) / (\cos \alpha_2 \tan \alpha_1 - \sin \alpha_2) \quad (22)$$

$$a_{str1} = (a_b - a_{str2} \cos \alpha_2) / \cos \alpha_1 \quad (23)$$

where bond length (l_{n2}) is limited by $(a_c - a_b \tan \alpha_1)$. Thereby, the effective strength of C-C-C node is expressed as:

$$V_{N2} = a_{str1} b f_{cd} \cos \alpha_1 + (a_{str2} b (0.85 f'_c) + n\pi d_b l_{n2} f_{bc}) \cos \alpha_2 \quad (24)$$

Equilibriums and shear strength of joint

From the equilibrium condition of the forces joined at nodes within the upper chord, the horizontal shear force from the strut-and-tie model is found.

$$V_u = D_1 \cos \alpha_1 + D_2 \cos \alpha_2 + V_T \quad (25)$$

where, the first and second terms of the right side mean the shear force transferred by diagonal strut mechanism including the confining effect of joint reinforcement, while third term means that of the truss mechanism.

Using the effective strengths to be defined above, the limit of each component (D_1 , D_2 , and V_T) can be determined. Firstly, the shear force resisted by the truss mechanism is limited by the strength of T-T-C node ($N1$) and the strengths of horizontal and vertical ties.

$$V_T = \min. \text{ of } \begin{cases} n\pi d_b l_{n1} f_b \\ A_{sh} f_y \\ A_{sv} f_y \tan \alpha_1 \end{cases} \quad (27)$$

The limit of direct diagonal strut D_1 force is determined by the effective strength of cracked concrete as:

$$D_1 = a_{str1} b f_{cd} \quad (26)$$

The maximum of strut D_2 is limited not only by the effective strength of cracked concrete but also by the remainder of horizontal tie force and the effective strength of C-C-C node ($N2$).

$$D_2 = \min. \text{ of } \begin{cases} (h_c - 2a_c + a_{str2} + l_{n2} \sin \alpha_2) b f_{cd} / 2 \cos \alpha_2 \\ (A_{sh} f_y - V_{N1}) / \cos \alpha_2 \quad (\geq 0) \\ a_{str2} b (0.85 f'_c) + n\pi d_b l_{n2} f_{bc} / \cos \alpha_2 \end{cases} \quad (27)$$

VERIFICATION

Test specimens described in literatures [8][9][10][11][12][13][14] are investigated to verify the proposed model. All specimens are designed to have the column strength higher than the beam strength to cause the plastic hinges at the beams. Fig. 7 shows definitions of geometries of the specimens of internal beam-column joints for the analysis with the proposed strut-and-tie model. Geometries of specimens, material properties and axial loading above column are summarized in Table 1.

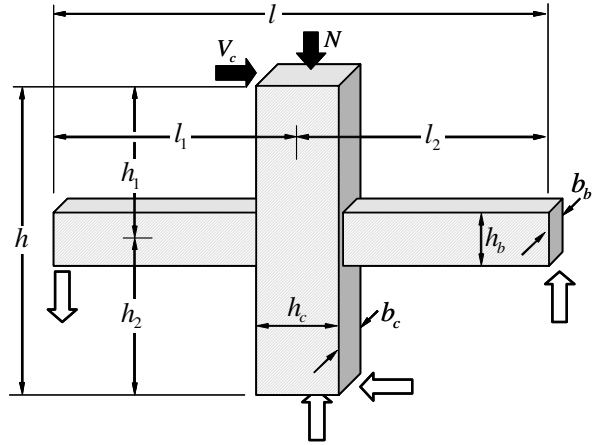


Fig. 7 Definitions of Geometries of interior beam-column joint

In all the test data, the deformation of beam-column assemblage is represented as inter-story drift (Δ) or drift angle (R). To compare the calculated results by the proposed model with test data, it precedes to find the relationship between the main bar strain of the beam (ϵ_{req}) representing the plastic deformation in the proposed model and the inter-story drift shown in test. Fig. 8 shows the deformation of interior beam-column assemblage comprising (a) elastic deformation of beams and columns, (b) plastic deformation of beam plastic hinge, and (c) shear deformation of joint itself. Accordingly, inter-story drift (Δ) and drift angle (R) of interior beam-column joint are

$$\Delta = \Delta_{C1} + \Delta_{C2} + \left(\Delta_{Be1} + \Delta_{Be2} + \Delta_{Bp1} + \Delta_{Bp2} \right) \frac{h}{l} + \gamma_J h \quad (28)$$

$$R = \Delta/h \quad (29)$$

where, Δ_{C1} , Δ_{C2} , Δ_{Be1} and Δ_{Be2} are elastic deformations of columns and beams, respectively; Δ_{Bp1} and Δ_{Bp2} are plastic deformation of right and left beams; h and l are the height and length of beam-column assemblage, respectively; γ_J is average shear strain of the joint.

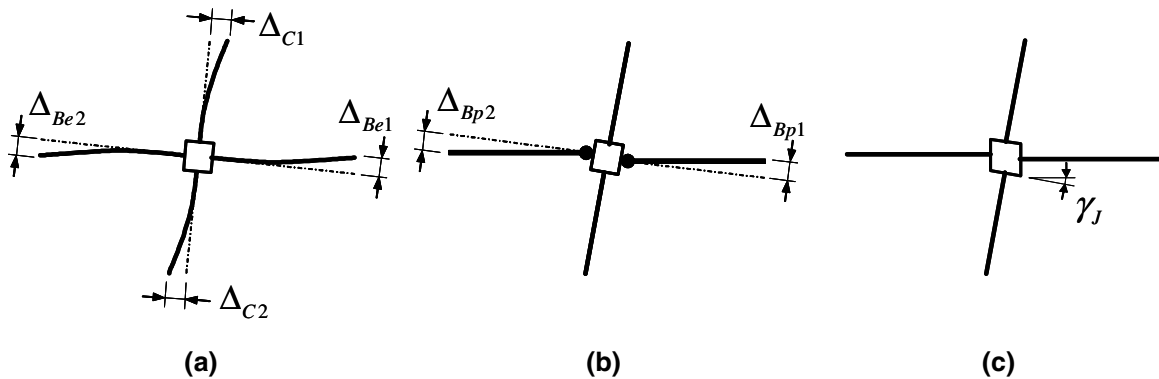


Fig. 8 Relationships of Inter-story drift and member deformations (a) elastic deformation of beam and column (b) plastic hinge deformation (c) Joint shear deformation

Table 1. Test parameters of interior beam-column joint

Authors	Specimens	$l^{(1)}$ (mm)	$h^{(2)}$ (mm)	h_b (mm)	b_b (mm)	h_c (mm)	b_c (mm)	f'_c (MPa)	$A_{s1}f_y$ (kN)	$A_{s2}f_y$ (kN)	$A_{sh}f_y$ (kN)	$A_{sv}f_y$ (kN)	$N^{(3)}$ (kN)
Joh et al. [8]	HH	3000	1750	350	200	300	300	25.6	161	161	457	322	353
	HL	3000	1750	350	200	300	300	27.4	161	161	457	322	353
	MH	3000	1750	350	200	300	300	28.1	161	161	107	322	353
	LH	3000	1750	350	200	300	300	26.9	161	161	64	322	353
Fujii et al. [9]	A1	2000	1500	250	160	220	220	40.2	257	257	49	513	147
	A2	2000	1500	250	160	220	220	40.2	257	257	49	308	147
	A3	2000	1500	250	160	220	220	40.2	257	257	49	513	441
	A4	2000	1500	250	160	220	220	40.2	257	257	132	513	441
Kitayama et al. [10]	J1	2700	1470	300	200	300	300	25.7	426	213	62	319	176
	C1	2700	1470	300	200	300	300	25.6	302	151	55	336	176
	B1	2700	1470	300	200	300	300	24.5	394	394	53	590	176
	B2	2700	1470	300	200	300	300	24.5	293	293	140	389	176
Leon.[11]	BCJ2	2134	1464	305	203	254	254	30.3	227	128	53	341	0
	BCJ3	2032	1464	305	203	254	305	27.4	227	128	53	341	0
	BCJ4	1930	1464	305	203	254	356	27.2	227	128	53	227	0
Li. et al. [12]	A1	4000	2500	600	300	300	900	32.3	506	303	0	0	0
	A2	4000	2500	600	300	900	300	32	880	452	301	1355	0
	M1	4000	2500	600	300	300	900	32.5	506	303	0	0	0
	M2	4000	2500	600	300	900	300	30.3	880	452	301	1355	0
Filiatrault et al. [13]	S1	3920	3500	500	400	400	400	39	565	283	126	754	670
	S2	3920	3500	500	400	400	400	46	565	283	503	754	670
Lin. [14]	Unit 1	3190	2450	550	300	390	390	33.3	475	475	480	417	1800
	Unit 2	3190	2450	550	300	390	390	33.3	475	475	721	417	1800
	Unit 3	3190	2450	550	300	390	390	37	356	356	320	417	450
	Unit 4	3190	2450	550	300	390	390	37	475	238	320	417	450
	Unit 8	3190	2450	550	300	390	390	33.2	475	475	556	417	450

⁽¹⁾ overall beam length (l_1+l_2) ⁽²⁾ overall column length (h_1+h_2) ⁽³⁾ Axial force acting on column

Elastic deformations of beams and columns can be calculated with effective stiffness ($E_c I_{eff}$) of RC flexural members suggested by ACI [1].

$$\Delta_{Ci} = \frac{V_c (h_i - h_b / 2)^3}{3E_{col} I_{col}} \quad (30)$$

$$\Delta_{Bej} = \frac{V_{Bj} (l_j - h_c / 2)^3}{3E_{Beam} I_{Beam}} \quad (31)$$

where, subscript i takes 1 in upper column and 2 in lower column; $E_{col} I_{col}$ is effective stiffness of column; subscript j takes 1 in left beam and 2 in right beam; $E_{beam} I_{beam}$ is effective stiffness of beam; and V_c and V_b are shear force of column and beam, respectively at the flexural yielding of beam.

The plastic deformation of beam is determined with plastic strain (ϵ_p) and plastic hinge length (l_p).

$$\Delta_{Bpj} = \frac{\varepsilon_p}{h_b - a_b} l_p \left(l_j - \frac{h_c}{2} - \frac{l_p}{2} \right) \quad (32)$$

Table 2. Verification of proposed model with experimental results

Authors	Specimens	Test results		Results from proposed model				V_c (cals/test)	R_{max} (cals/test)
		V_c (kN) ⁽¹⁾	R_{max} ⁽²⁾	V_c (kN) ⁽³⁾	V_{jh} (kN) ⁽⁴⁾	$V_{u,ini}$ (kN) ⁽⁵⁾	$R_{max,cal}$ ⁽⁶⁾		
Joh et al. [8]	HH	63.5	0.032	59.9	262	396	0.035	0.94	1.09
	HL	64.8	0.025	59.8	262	398	0.036	0.92	1.44
	MH	62.9	0.025	59.9	262	318	0.014	0.95	0.56
	LH	65.4	0.029	59.7	262	298	0.013	0.91	0.45
Fujii et al. [9]	A1 [∇]	66.7	0.030	72.8	441	332	-	1.09	-
	A2 [∇]	61.5	0.046	72.8	441	332	-	1.18	-
	A3	66.7	0.031	72.8	441	423	-	1.09	-
	A4	68	0.031	72.8	441	463	0.018	1.07	0.58
Kitayama et al. [10]	J1 [∇]	108	0.040	108.5	530	365	-	1.00	-
	C1	98	0.029	80.8	372	326	-	0.82	-
	B1 [∇]	128	0.037	125.2	663	456	-	0.98	-
	B2 [∇]	118	0.041	98.6	488	455	-	0.84	-
Leon. [11]	BCJ2 [∇]	49.1	0.039	41.5	313	221	-	0.85	-
	BCJ3 [∇]	55.5	0.034	41.5	313	210	-	0.75	-
	BCJ4 [∇]	67.4	0.031	41.8	313	210	-	0.62	-
Li. et al. [12]	A1 [∇]	162.4	0.013	176	632	307	-	1.08	-
	A2	322.1	0.016	333	998	1161	0.013	1.03	0.81
	M1 [∇]	188.7	0.012	176	632	308	-	0.94	-
	M2	389.7	0.015	331	1000	1133	0.012	0.85	0.8
Filiatrault et al. [13]	S1	151	0.02	138	922	820	-	0.91	-
	S2	158	0.028	139	922	1020	0.021	0.88	0.75
Lin. [14]	Unit1	225	0.026	204	746	1144	0.033	0.91	1.27
	Unit2	225	0.028	204	746	1227	0.05	0.91	1.78
	Unit3	170	0.02	156	556	655	0.015	0.92	0.75
	Unit4	175	0.025	155	557	610	0.015	0.89	0.6
	Unit8	220	0.04	204	746	824	0.025	0.39	0.63

⁽¹⁾ maximum shear force of column loaded in test ⁽²⁾ story drift angle at maximum shear force in test
⁽³⁾ column shear force after beam plastic hinge occurring, third term of right side in Eq. (2) ⁽⁴⁾ horizontal joint shear force after beam plastic hinge occurring, calculated by Eq. (2) ⁽⁵⁾ horizontal shear strength of joint at $R=0$ ⁽⁶⁾ story drift angle at $V_u=V_{jh}$
[∇] means the specimen shows failure before beam plastic hinge occurred in test. ($V_{u,ini} < V_{jh}$)

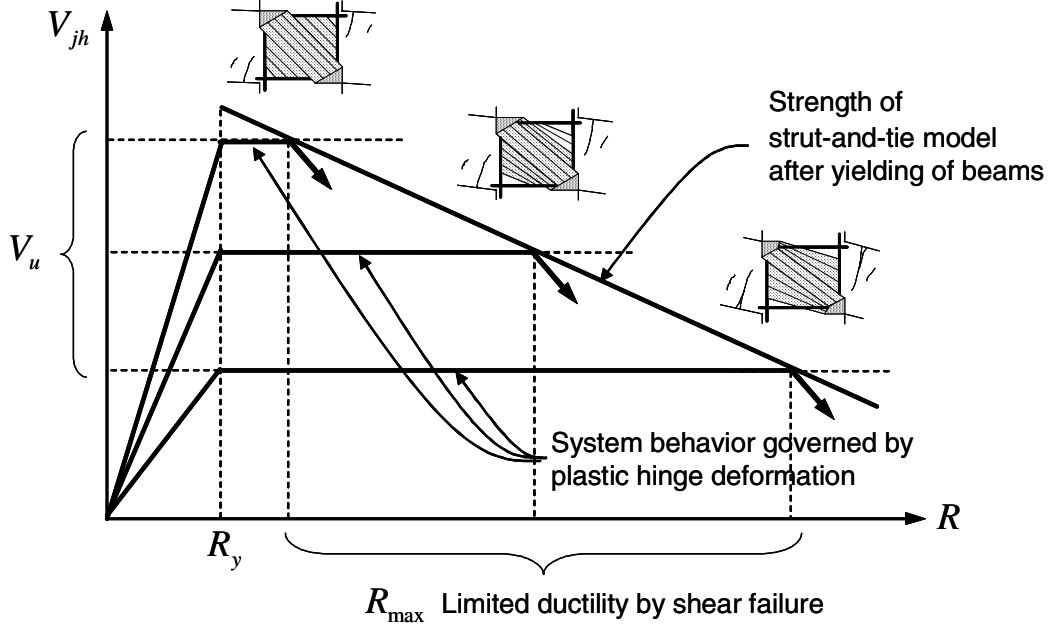


Fig.10 Behavior and strength of interior beam-column joint involving a plastic hinge

where subscript j takes 1 in left beam and 2 in right beam; plastic hinge length (l_p) is taken as the simple approximated value ($l_p = 0.5h_b$) by Pauley and Priestley [2].

Shear deformation of the joint is simply approximated with the strain of horizontal tie and diagonal strain as shown in Fig. 9.

$$\gamma_j = \frac{\epsilon_c}{\cos^2 \alpha_1} + \epsilon_h \quad (33)$$

Finally, the required strain of beam bars at column face (ϵ_{req}) is

$$\epsilon_{req} = \epsilon_p + \epsilon_y \quad (34)$$

The shear strength of an interior beam-column joint (V_u) decreases as the story drift angle (R) increases, while the internal horizontal shear forces within the joint (V_{jh}) remain constant after both beams yield. A conceptual relationship between the joint strength and the system ductility is illustrated in Fig. 10. The intersection point of the two curves (R_{max}) indicates the system ductility limited by the shear failure of beam-column joint.

Test results and the calculation from the proposed model are listed in Table 2 with the comparisons of column shear (V_c) and story drift angle at failure (R_{max}). Some of the joints show the failure before their beam plastic hinges are developed, which are identified from the

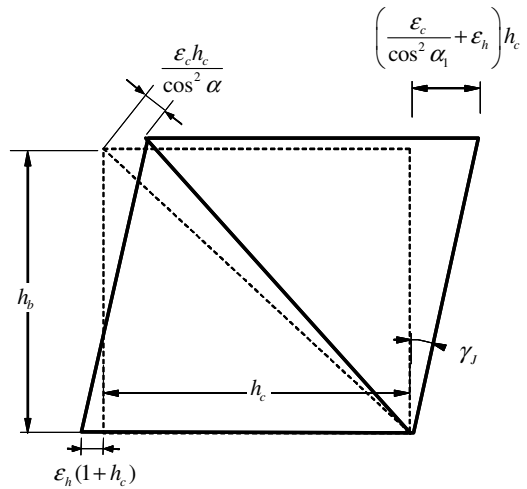


Fig. 9 Shear deformation of joint

comparison of V_{jh} (horizontal joint shear strength under the assumption of beams yielding) with initial strength of joint V_{ini} (shear strength of joint when the story drift has zero value). The results calculated from the proposed model show good agreements with test results.

CONCLUSIONS

Strut-and-tie models for determining the shear strengths of interior beam-column joints dependent on the deformation conditions are proposed. To determine the strength of the proposed strut-and-tie models, the effective strengths of the components that comprise struts, ties, C-C-C nodes, and T-T-C nodes, are postulated in accordance with the bond deterioration and the concrete softening, which depend mainly on the plastic hinge behavior of beams.

Since the proposed models are dependent on the deformation conditions, they can provide a clearer understanding of the loading path within the interior beam-column joints, which varies with the plastic response of the system. These deformation dependent strut-and-tie models can be used as rational tools for evaluation of existing joints and for the design not only in high seismicity zone but low- or mid- seismicity zones where fully ductile behavior is not required.

REFERENCES

1. ACI Committee 318, Building Code Requirements for Structural Concrete and Commentary (ACI 318-98 / ACI 318R-98), American Concrete Institute, Farmington Hills, Michigan, 1998.
2. Park, R., and Pauley, T., "Reinforced Concrete Structures", John Wiley and Sons, 1975: 738-742.
3. Hwang, S. J. and Lee, H. J., "Analytical Model for Predicting Shear Strength of Exterior Reinforced Concrete Beam-Column Joints for Seismic Resistance", ACI Structural Journal, 1999, 96 (5): 846-858.
4. Hwang, S. J. and Lee, H. J., "Analytical Model for Predicting Shear Strength of Interior Reinforced Concrete Beam-Column Joints for Seismic Resistance", ACI Structural Journal, 2000, 97 (1): 35-44.
5. Paulay, T., and Priestley, M. J. N., "Seismic Design of Reinforced Concrete and Masonry Buildings", John Wiley & Sons, Inc., 1992: 744
6. Vecchio, F. J., and Collins, M. P., "Modified Compression-Field Theory for Reinforced Concrete Elements Subjected to Shear," ACI Structural Journal, 1996, 83 (2): 219-231.
7. Hsu, T. T. T., "Softened Truss Model Theory for Shear and Torsion" ACI Structural Journal, 1998, 85 (6): 624-635.
8. Joh, O., Goto, Y., and Shibata, T., "Influence of Transverse Joint and Beam Reinforcement and Relocation of Plastic Hinge Region on Beam-Column Joint Stiffness Deterioration," Design of Beam-Column Joints for Seismic Resistance, SP-123, ACI, 1991: 187-224.
9. Fujii, S., and Morita, S., "Comparison between Interior and Exterior Beam-Column Joint Behavior," Design of Beam-Column Joints for Seismic Resistance, SP-123, ACI, 1991: 145-165.
10. Kitayama, K., Otani, S., and Aoyama, H., "Development of Design Criteria for RC Interior Beam-Column Joints", Design of Beam-Column Joints for Seismic Resistance, SP-123, ACI, 1991: 97-123.
11. Leon, R. T., "Shear Strength and Hysteretic Behavior of Interior Beam-Column Joints," ACI Structural Journal, 1990, 87 (1): 3-11.
12. Li, B., Wu, Y., and Pan, T. C., "Seismic Behavior of Nonseismically Detailed Interior Beam-Wide Column Joints - Part I: Experimental Results and Observed Behavior," ACI Structural Journal, 2002, 99 (6): 791-802.
13. Filiatrault, A., Pineau, S., and Houde, J., "Seismic Behavior of Steel-Fiber Reinforced Concrete Interior Beam-Column Joints," ACI Structural Journal, 1995, 92 (5): 543-552.

14. Lin, C. M., "Seismic Evaluation and Design of Reinforced Concrete Interior Beam Column Joint", Research Report 2000-1, Department of Civil Engineering, University of Canterbury, Christchurch.